The Q-Loop of DrrA Is Involved in Producing the Closed Conformation of the Nucleotide Binding Domains and in Transduction of Conformational Changes between DrrA and DrrB[†]

Divya K. Rao and Parjit Kaur*

Department of Biology, Georgia State University, Atlanta, Georgia 30303

Received August 21, 2007; Revised Manuscript Received January 4, 2008

ABSTRACT: DrrA and DrrB proteins form an ATP-dependent efflux pump for doxorubicin and daunorubicin in *Streptomyces peucetius*. DrrA, the catalytic subunit, forms a complex with the integral membrane protein DrrB. Previous studies have provided evidence for strong interaction between these two proteins, which was found to be critical for binding of ATP to DrrA and for stability of DrrB. Chemical cross-linking experiments carried out previously showed that in the resting state of the complex DrrA and DrrB are in contact with each other. Use of a cysteine-to-amine cross-linker then allowed identification of the N-terminal cytoplasmic tail of DrrB (residues 1–53) as the primary region of contact with DrrA. In this study, single-cysteine substitutions were introduced into different domains of DrrA in a strain already containing the S23C substitution in the N-terminal tail of DrrB. By using different arm-length disulfide cross-linkers, we found that a cysteine placed in the Q-loop region of DrrA traps DrrA in the dimeric state, thus indicating that in the closed conformation the Q-loops from opposing subunits are in the proximity of each other. Furthermore, the same region of DrrA was also found to interact with the N-terminus of DrrB, although the A−A interaction was much more prominent than the A−B interaction under these conditions. On the basis of additional data shown here, we propose that the interaction of the Q-loop with the N-terminal cytoplasmic tail of DrrB identifies an important step in the communication of conformational changes between DrrA and DrrB. The significance of these findings in the mechanism of the DrrAB complex is discussed, and a model based on analyses of different conformations of DrrA and DrrB is presented.

Self-resistance to doxorubicin and daunorubicin, two anticancer antibiotics, in the producer organism *Streptomyces peucetius* is conferred by DrrA and DrrB proteins (*1*). Together, these two proteins are proposed to form an ATP-driven drug pump for the export of these antibiotics, in the process conferring resistance (*1, 2*). We are interested in understanding the mechanism by which this prototype drug transporter carries out efflux of these antibiotics. This is important for a variety of reasons, the most important being that drug resistance is an emerging clinical problem and an understanding of the mechanism of resistance can help in designing effective strategies to combat drug resistance. Furthermore, the DrrAB system exhibits similarities with P-glycoprotein (Pgp),[1] an MDR protein overexpressed in cancer cells. Pgp confers multidrug resistance by carrying out ATP-dependent efflux of a variety of structurally unrelated drugs, including doxorubicin and daunorubicin (*3*). Both DrrAB and Pgp also belong to the ABC family of proteins; therefore, they share not only functional but also sequence similarity. Thus, the DrrAB system can shed light on the mechanism and origin of multidrug resistance.

Most ABC transporters are composed of four domains: two transmembrane (TMD) and two nucleotide binding domains (NBD). In Pgp, all four domains are present on a single polypeptide (*3–5*), while in DrrAB, the domains are present on separate subunits (*1, 2, 6–8*). The functional complex of DrrAB is believed to consist of two subunits of DrrA and two of DrrB (*6*). Crystal structure data for several ABC proteins and intact ABC transporters are now available (*9–23*). These structures depict the structure of an NBD monomer to be L-shaped having two arms (*9–17*). Arm I contains the Walker A and Walker B motifs and is known as the RecA-like core ATP domain, while arm II contains the signature motif as part of the α-helical domain. A flexible Q-loop, which contains a highly conserved glutamine at its N-terminus, joins the RecA-like core domain to the α-helical domain. More recently determined crystal structures, especially of *Escherichia coli* MalK (*19*) and *Methanococcus jannaschii* MJ0796 proteins (*11*), have also facilitated identification of the head-to-tail dimeric intermediates of the NBDs. In a head-to-tail dimer, the Walker A domain of one subunit is aligned with the signature domain from the opposing subunit, thus producing two nucleotide binding

[†] This work was supported by National Institutes of Health Service Award RO1 GM51981-09.

* To whom correspondence should be addressed. E-mail: pkaur@gsu.edu. Telephone: (404) 413-5405. Fax: (404) 413-5301.

[1] Abbreviations: Pgp, p-glycoprotein; MDR, multidrug resistance; NBD, nucleotide binding domain; TMD, transmembrane domain; CuPhe, copper phenanthroline; DTME, dithiobismaleimidoethane; MTS, 3,6,9,12,15-pentaoxaheptadecane-1-methanethiosulfonate; GMBS, *N*-(γ-maleimidobutyryloxy)succinimide ester; NBD-Cl, 7-chloro-4-nitrobenzo-2-oxa-1,3-diazole; MIANS, 2-(4′-maleimidylanilino)naphthalene-6-sulfonic acid; FRET, Fourier resonance energy transfer.

10.1021/bi701699a CCC: $40.75
Published on Web 02/01/2008

interfaces in a dimer. This conformation is achieved in the presence of ATP and is termed the closed conformation. In the nucleotide-free or open conformation, the NBDs are no longer in the proximity of one another (*19*). In the crystal structure of Sav1866, an MDR protein from *Streptomyces aureus*, constraints on the structure, which might result from domain swapping, have been noted. This might imply a more limited movement of the NBDs as compared to the predictions from other structures (*23*). Although availability of structural data from many different ABC proteins (both soluble and intact transporters) has already provided many important insights, still crystal structures present only snapshots. The biochemical characterization of these and other ABC transporters will thus be essential in complementing structural studies and developing a full understanding of the mechanisms by which energy is transduced between the ABC domains and the transmembrane domains. Characterization of the DrrAB drug export system can therefore provide a valuable understanding of the efflux systems, especially drug efflux systems.

The *drrAB* locus of *S. peucetius* has been subcloned, and the proteins have been expressed in *E. coli* (*2*). The expression of these two proteins confers doxorubicin resistance in this host, indicating that the complex is assembled properly (*2*). Initial characterization of this system showed that DrrB is an integral membrane protein, and it contains eight transmembrane helices (*8*). DrrA, a peripheral membrane protein, forms a complex with DrrB in the cell membrane, and it functions as the catalytic subunit (*2*). Furthermore, DrrA and DrrB are biochemically dependent on each other for stability and function (*6*). For example, DrrA binds ATP/GTP only if it is in a complex with DrrB in the membrane, and DrrB is unstable if DrrA is absent. While many of these factors make the study of this system quite challenging, at the same time, because of its separate subunit architecture and tight intersubunit interactions, it makes for an ideal system for studying NBD−NBD and NBD−TMD interactions.

In a recent study conducted in this laboratory, we introduced several single-cysteine substitutions into DrrB and then by using a cysteine-to-amine heterobifunctional cross-linker showed that DrrA interacts predominantly with the N-terminal cytoplasmic tail (residues 1–53) of DrrB (*7*). Within this region of DrrB, we also identified a sequence with similarities to the EAA motif found in importers of the ABC family of proteins, thus leading to the proposal that the EAA or EAA-like motif may be involved in forming a generalized interface between the ABC and the TMD of both uptake and export systems. The goal of this study was to characterize DrrA and to further our understanding of interactions between DrrA and DrrB. By using a combination of approaches, including point mutations, cysteine substitutions in the conserved domains of DrrA, and disulfide cross-linking analysis, we show here that the Q-loop region of DrrA plays an important role in dimerization of DrrA as well as in interactions with DrrB. We provide evidence showing that DrrA can be trapped in the closed conformation by placing a cysteine substitution in the Q-loop region, thus indicating that in the closed state two Q-loops from opposing subunits are in the proximity of each other. Furthermore, we also show that the interaction of the Q-loop with the N-terminus of DrrB is involved in transmitting conformational changes between DrrA and DrrB. Implications of these findings in the mechanism of the DrrAB complex are discussed, and a model depicting different conformations of DrrA and DrrB is presented. While this manuscript was being completed, a similar study carried out with the maltose system was published (*24*). This study also shows that the distance between the Q-loops of MalK is significantly reduced when the protein is in the closed state, thus supporting the conclusions of our study as well as the previous crystal structure analysis of MalK (*17, 19, 24, 25*). Findings of this study will also be discussed.

EXPERIMENTAL PROCEDURES

Bacterial Strains and Plasmids. The following bacterial strains were used in this study: *E. coli* TG1 (*26*), N43 (*25*), HMS174 (*26*), and XL1 Blue (*26*). The plasmids used in this study included pDX101 (*drrAB* in pSU2718), pDX132 (*drrA* in pET16b), and pDX121 (*drrAB* in pET28a). Different mutations and substitutions of the *drrA* or *drrB* gene were created in these clones.

Media and Growth Conditions. The cells were grown in LB medium (*27*) at 37 °C, unless mentioned otherwise. Chloramphenicol was added to a final concentration of 20 μg/mL, and kanamycin was added to a final concentration of 30 μg/mL, where needed.

Site-Directed Mutagenesis of drrA. Single- and double-cysteine variants of DrrA were constructed by site-directed mutagenesis using a strategene QuikChange multi-site-directed mutagenesis kit (Stratagene, La Jolla, CA). The strategy involved the use of complementary primers that incorporated the change at the required position. The templates used included pDX101 and pDX121, and the primers were designed as described previously (*7*). The single cysteine present in DrrB was first mutagenized to serine (C260S). Cysteine substitution mutants were then created at amino acid positions 45, 89, 140, 174, 195, and 198 in DrrA. These mutants were named A45C(A)/C260S(B), Y89C(A)/C260S(B), Y140C(A)/C260S(B), S174C(A)/C260S(B), T195C(A)/C260S(B), and Y198C(A)/C260S(B). For double-cysteine mutants, cysteine substitutions of DrrA were created in the DrrB S23C background. Double substitutions were created at amino acid positions 89, 91, 174, 195, and 198 of DrrA. These mutants were named Y89C(A)/S23C(B), S91C(A)/S23C(B), S174C(A)/S23C(B), T195C(A)/S23C(B), and Y198C(A)/S23C(B). Conservative and non-conservative point mutations in certain residues in different domains of DrrA were also made. These changes include G44S, G44A, K47E, and K47R (Walker A), L160A, D164A, and E165Q (Walker B), Q88E, Q88S, and Q88N (Q-loop), and S141R and G143S (signature domain).

Doxorubicin Resistance Assay. Doxorubicin resistance assays were carried out on M9 (*26*) plates supplemented with 0.25% casamino acids. The plates were layered with 4 mL of top agar (0.8% agar in M9 medium) containing the desired concentration of doxorubicin. Briefly, 4 mL of top agar containing 0, 6, 8, or 10 μg/mL doxorubicin (Sigma Chemicals) and 1 mM thiamine-HCl was poured on top of M9 plates. The plates were covered with foil to prevent exposure to light. N43, a doxorubicin-sensitive strain of *E. coli*, was transformed with the indicated plasmids. Freshly transformed cells were grown for 8 h in 3 mL of LB with

the appropriate antibiotics. One microliter of the 8 h old N43 culture from above was streaked on plates containing doxorubicin. N43 containing the plasmid pSU2718 was used as a negative control. The plates were then incubated at 37 °C overnight, and growth was recorded after incubation for 24 h.

Nucleotide Binding Properties of DrrA Mutants. To study nucleotide binding, photolabeling of the various mutants of DrrA with [α-^{32}P]ATP was carried out (*2, 6*). A 50 mL culture of *E. coli* TG1 cells containing the indicated plasmids was grown to midlog phase and induced with 0.25 mM IPTG. Growth was continued for an additional 3 h at 37 °C. The cells were spun down and resuspended in 1.5 mL of QAE buffer [25 mM Tris-HCl (pH 8.0), 20% glycerol, and 2 mM EDTA] containing 1 mM DTT and lysed by a single passage through a French pressure cell at 20000 psi. The cell lysates were then centrifuged at 10000*g* for 15 min to remove unbroken cells. The supernatant was centrifuged at 100000*g* for 1 h to prepare membrane protein. An ATP binding assay was carried out in a 100 μL reaction volume containing 0.1 mg of membrane protein, 25 mM Tris-HCl (pH 8.0), 20% glycerol, 2 mM EDTA, 10 μM ATP, 250 μM Mg^{2+}, 35 μM doxorubicin, and 10 μCi of [α-^{32}P]ATP. The mixture was exposed to UV light at 254 nm for 30 min on ice. Proteins were precipitated with 400 μL of 10% TCA on ice for 30 min. Samples were spun down at 14000*g* for 15 min, and the pellet was resuspended in 20 μL of 4× Laemmli sample buffer containing 5 μL of 1 M unbuffered Tris. The samples were solubilized by being heated at 55 °C for 10 min and analyzed by SDS−PAGE using a 10% polyacrylamide gel, followed by autoradiography.

Purification of Wild-Type and Mutant DrrAB Proteins. DrrAB proteins were purified using pDX121, which introduces His tags at the N-terminus of DrrA and the C-terminus of DrrB. DrrA was purified using pDX132, which introduces a His tag at the N-terminus of DrrA. HMS174 cells containing the indicated plasmid were induced with IPTG. Membrane and cytosolic fractions were prepared as described above. DrrA protein was purified from the cytosolic fraction by using a Ni-NTA column, while the DrrAB proteins were solubilized from the membrane fraction and purified as a complex using Ni-NTA. For solubilization, 5 mg of membrane protein was incubated in 5 mL of buffer [KP_i (pH 7.4), 200 mM NaCl, and 20% glycerol] containing 1 mM DTT, 1× protease cocktail (Roche), and 1% *n*-octyl glucoside (*n*-OG) on ice for 1 h. This was followed by ultracentrifugation at 100000*g* for 1 h, and the supernatant was loaded on the Ni-NTA column. The elution of the DrrAB complex was carried out with the same buffer mentioned above containing 1% *n*-OG and 500 mM imidazole. The indicated amounts of proteins were analyzed by SDS−PAGE using a 10% polyacrylamide gel, followed by Western blot analysis with anti-DrrA antibodies.

Homobifunctional (disulfide) and Heterobifunctional (cysteine-to-amine) Cross-Linking. For homobifunctional cross-linking, a 100 μL reaction volume containing 250 μg of membrane protein in 0.1 M phosphate buffer (pH 7.4) was treated with thiol-specific reagents copper phenanthroline (CuPhe) (3 mM $CuSO_4$ and 9 mM 1,10-phenanthroline), DTME (dithiobismaleimidoethane) (1 mM) (Pierce Chemicals), or MTS (3,6,9,12,15-pentaoxaheptadecane-1-methanethiosulfonate) (0.2 mM) (Toronto Research Chemicals) for 30 min at room temperature. For heterobifunctional cross-linking, a 100 μL reaction volume containing 250 μg of membrane protein in 0.1 M phosphate buffer (pH 7.4) was treated with GMBS [*N*-(γ-maleimidobutyryloxy)succinimide ester] (1 mM) (Pierce Chemicals) for 1 h at room temperature in a light-protected area. The reactions were terminated by the addition of 25 μL of 4× nonreducing Laemmli sample buffer. The samples were mixed thoroughly and set aside for 5 min at room temperature. A 25 μL portion (50 μg of membrane protein) of the reaction mixture was then analyzed by SDS−PAGE using a 10% polyacrylamide gel, followed by Western blot analysis using either anti-DrrA or anti-DrrB antibodies. To study the effect of ATP and ATPγS on cross-linking, 35 μg of purified wild-type or mutant DrrAB proteins was incubated in a 100 μL reaction volume containing 0.1 M phosphate buffer (pH 7.4) with or without 10 mM ATPγS, 10 mM ATP, or 1 mM DTME for 30 min at room temperature. Where indicated, the purified proteins were (prior to incubation) reduced with 1 mM DTT and immediately passed through a 10K Nanosep centrifugal column (Pall Corp.) to remove DTT. The samples were resuspended in 0.1 M phosphate buffer (pH 7.4); 35 μg of the reduced protein was then incubated in a 100 μL reaction volume with ATPγS, ATP, or DTME, as described above. The reaction was terminated by the addition of 4× nonreducing Laemmli sample buffer. Fifteen micrograms of protein was analyzed by SDS−PAGE, followed by Western blot analysis.

Determination of the Composition of the 78 kDa Cross-Linked Species by SELDI. DrrAB proteins containing a cysteine at position 89 in DrrA [Y89C(A)/C260S(B)] were purified by using a Ni-NTA column. The purified sample was subjected to disulfide cross-linking using DTME as described above. The samples were analyzed by SDS−PAGE using a 10% polyacrylamide gel, followed by Coomassie Blue staining (*26*). The band of interest was excised and subjected to in-gel digestion with 100 ng of trypsin. The mass of the trypsin-generated peptide fragments was determined by surface-enhanced laser desorption/ionization (SELDI) using the CIPHERGEN Protein Chip Technology in the core facility of the Department of Biology at Georgia State University.

Fourier Resonance Energy Transfer (FRET). In separate reactions, 5 mg of membrane protein prepared from A45C(A)/C260S(B) or Y140C(A)/C260S(B) was incubated with either 1 mM NBD-Cl (7-chloro-4-nitrobenzo-2-oxa-1,3-diazole) for 2 h at 22 °C or 30 μM MIANS [2-(4′-maleimidylanilino)-naphthalene-6-sulfonic acid] for 30 min at 22 °C. Unreacted probes were quenched with 1 mM dithioerythritol (DTE), and the samples were passed through a desalting column (Zeba TM Desalt Spin column, Pierce). NBD- or MIANS-labeled DrrAB proteins were solubilized and purified from the cell membrane, as described earlier. For FRET analysis, 250 μL of MIANS-labeled, purified A45C(A)/C260S(B) (approximately 100 μg of protein) proteins was mixed with 250 μL of NBD-labeled, purified Y140C(A)/C260S(B) and the mixture incubated for 30 min at 22 °C to obtain doubly labeled MIANS-NBD-A45C/Y140C DrrAB dimers. As controls, MIANS-labeled A45C(A)/C260S(B) was mixed with NBD-labeled A45C(A)/C260S(B) and MIANS-labeled Y140C(A)/C260S(B) was mixed with NBD-labeled Y140C(A)/C260S(B) for 30 min to obtain doubly

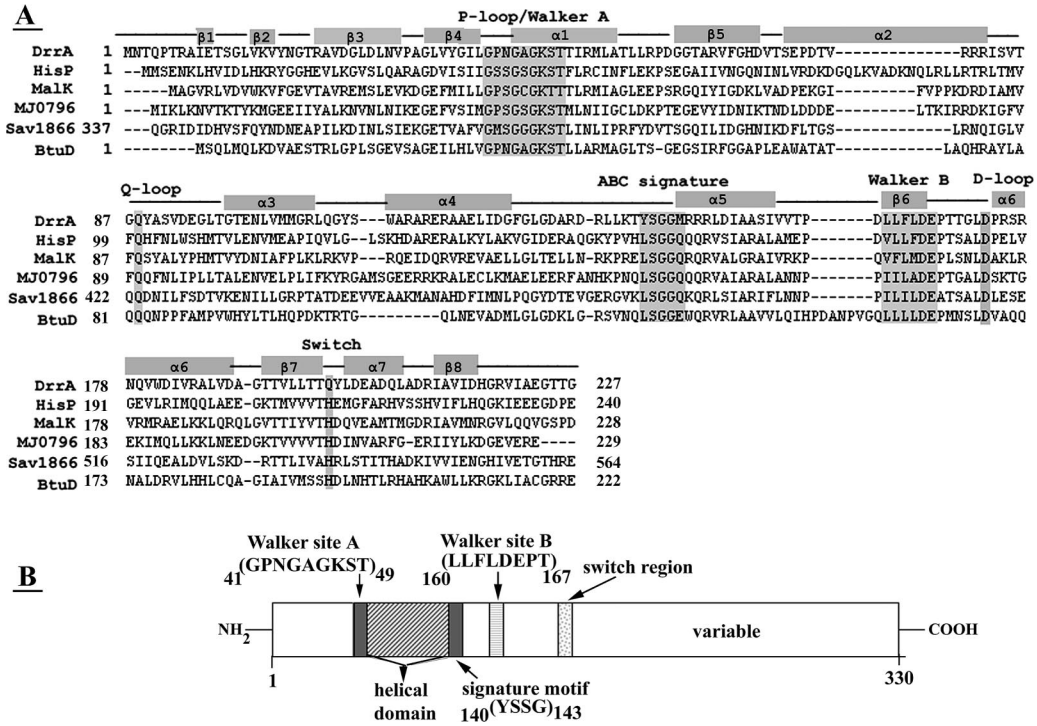

FIGURE 1: (A) Nucleotide binding domains of different ABC transporters. The alignment of DrrA, HisP, MalK, MJO796, Sav1866, and BtuD was generated by ClustalW (http://www.ebi.ac.uk/clustalw/). Secondary structure was predicted by the PHD tool obtained on the ExPASy server. Conserved domains mentioned in the text, namely, Walker A, Walker B, signature motif, and Q-loop, are highlighted in gray. Other highlighted domains include the D-loop and the switch region. (B) Schematic representation of the conserved domains in DrrA. The location, length, and consensus sequence of the Walker A domain, Walker B domain, signature motif, helical domain, and switch region are shown.

labeled MIANS-NBD-A45C DrrAB and MIANS-NBD-Y140C DrrAB, respectively. Fluorescence spectra were recorded on an Alphascan-2 spectrofluorimeter (Photon Technology International, London, ON). The excitation and emission slits were set at 4 nm. The excitation wavelengths for MIANS and NBD fluorophores were 322 and 465 nm, respectively, while emission was monitored at 420 and 523 nm, respectively, for individual probes. However, for the energy transfer experiment, samples were excited at 322 nm (for MIANS) while emission was monitored between 350 and 600 nm to include both MIANS and NBD.

RESULTS

Characterization of Point Mutations in DrrA. DrrA, the ABC subunit of the DrrAB pump, contains several conserved domains, as shown in the alignment of the amino acid sequence of DrrA with five other importers and exporters belonging to the ABC family (Figure 1A). The alignment was determined by ClustalW, and the secondary structure was analyzed by the PHD method of prediction. The alignment highlights the conserved domains within the ATPase domain of each transporter and shows the high degree of sequence similarity between each of them. These domains in DrrA are diagrammatically represented in Figure 1B. To study the effect of mutations within the conserved domains on the function of the DrrAB transporter, both conservative and nonconservative changes in residues within each domain were made. These include G44S, G44A, K47E, and K47R in the Walker A domain; L160A, D164A, and E165Q in the Walker B domain; Q88E in the Q-loop; and S141R and G143S in the signature motif. Protein expression analysis showed that mutations in the conserved domains caused varying degrees of reduction in the levels of DrrA and DrrB (Figure 2, left panels) as compared to the wild-type. Nucleotide binding properties of DrrA in each of these mutants were analyzed by [α-^{32}P]ATP cross-linking experiments. These data are shown in the right panels of Figure 2. As expected, Walker A mutations significantly reduced the level of binding of ATP to DrrA. E165Q, a Walker B mutant, however, showed high levels of ATP binding. Quantitation of these data and normalization to the levels of protein expression showed that the net amount of ATP bound to E165Q is slightly more than the amount of wild-type protein (Figure S1, panel A). The conserved glutamate in the Walker B domain is known to be crucial for hydrolysis of ATP but not for ATP binding; thus, the ATP binding phenotype observed for E165Q is consistent with that role. [Preliminary studies conducted in this laboratory have shown that the K_d for ATP binding in both wild-type and E165Q is in the range of 250–350 μM (data not shown).] A nonconservative mutation in the adjoining residue, D164A, showed a drastic reduction in expression levels of DrrA and DrrB and thus prevented ATP binding. Q88E mutation in the Q-loop reduced the level of ATP binding but did not completely abolish it, while the signature domain mutant, G143S, had no effect on binding of ATP. A nonconservative mutation, S141R, in the signature domain affected expression and completely abolished ATP binding.

It was previously shown that unlabeled ATP competes for binding of [α-^{32}P]ATP to wild-type DrrA (*2*). To determine if this is true for [α-^{32}P]ATP binding seen in the mutants, competition experiments using 10- and 50-fold higher concentrations of unlabeled ATP were carried out for K47R,

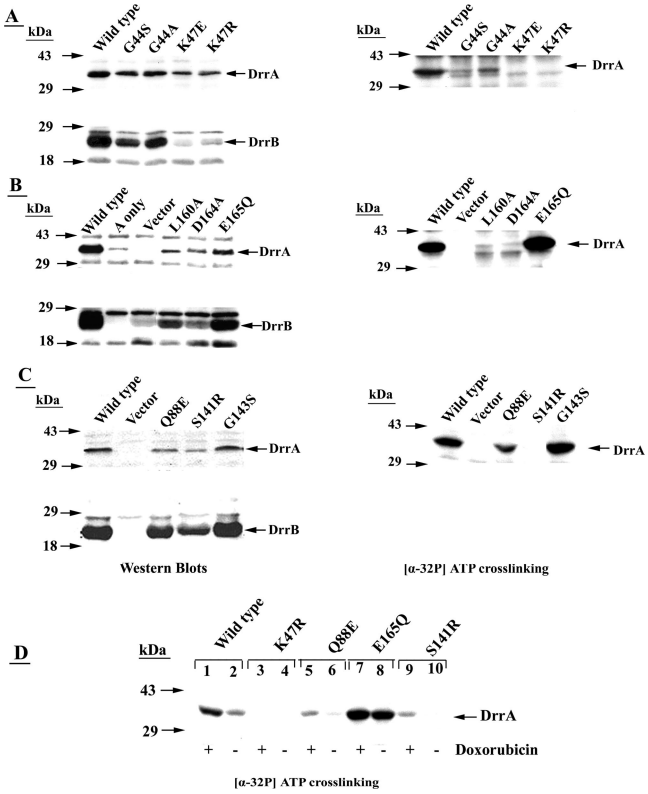

FIGURE 2: Effect of various mutations in DrrA on expression levels of DrrA and DrrB and on ATP binding. *E. coli* cells containing the indicated plasmids were induced with IPTG. The cells were lysed with a French press, followed by ultracentrifugation at 100000*g* for 1 h to prepare membrane fractions; 50 μg of membrane protein was analyzed by SDS−PAGE on 10% gels, followed by Western blot analysis using anti-DrrA (top) or anti-DrrB (bottom) antibodies. UV-catalyzed adduct formation between DrrA proteins and [α-^{32}P]ATP was performed as described in Experimental Procedures. Membrane proteins (100 μg) were resolved by SDS−PAGE on 10% gels, followed by autoradiography. (A−C) The reactions were carried out in the presence of 35 μM doxorubicin: (left) Western blots and (right) [α-^{32}P]ATP binding. (A) Walker A mutants. (B) Walker B mutants. (C) Q-Loop and signature motif mutants. (D) [α-^{32}P]ATP binding in the presence or absence of doxorubicin. Experimental conditions were the same as described for panels A−C. The samples marked with a plus sign contained 35 μM doxorubicin, while the samples marked with a minus sign contained no doxorubicin. The experiments shown in Figure 2 were repeated four times. The data obtained with key mutants (those used further in this work) were quantitated. The intensities of the bands in both Western blots (left) and the autoradiograms (right) were determined by densitometric scanning using Quantity one analysis software (Bio-Rad). The averages (from three or four experiments) of the ratio of ATP bound to protein concentration for selected mutants used for further experiments in this article are plotted in a histogram shown in Figure S1.

Q88E, E165Q, and S141R. Data in Figure S2 show that 10-fold higher concentration of unlabeled ATP is sufficient to completely prevent labeling with [α-^{32}P]ATP in all of the mutants tested. Finally, binding of ATP to DrrA is known to be stimulated by doxorubicin (*2*). The ATP binding experiments shown in panels A−C of Figure 2 were carried out in the presence of doxorubicin, as indicated in Experimental Procedures. The data in Figure 2D, however, show [α-^{32}P]ATP binding to a selected set of mutants both in the absence and in the presence of doxorubicin. These data show that doxorubicin stimulates binding of ATP to these mutants, which is seen with the wild-type protein. E165Q, however, binds ATP well even in the absence of doxorubicin, indicating that this mutation traps DrrA protein in the closed conformation. Quantitative data in panel B of Figure S1 show that the ratio of ATP bound in the absence to presence of doxorubicin in E165Q is higher (0.75) than that of the wild-type protein (0.45).

To determine if mutations in DrrA have an effect on the overall function of the transporter, doxorubicin resistance assays were carried out. The data show that while cells containing wild-type DrrA and DrrB grow up to 10 μg/mL doxorubicin (Table 1), the Q-loop mutant Q88E grows up to 6–8 μg/mL and all other mutants grow up to 4–6 μg/mL doxorubicin. Two nonconservative changes in the Q88 residue (Q88S and Q88N) were also tested. These two changes conferred much greater sensitivity to doxorubicin as compared to Q88E, implying an important role for the Q-loop in the function of the transporter. Some of the mutations described in Figure 2 were used in the following experiments described in this paper.

Head-to-Tail Conformation of DrrA Dimers. To determine if DrrA undergoes head-to-tail dimerization, as reported for other ABC proteins (*10, 11, 18, 19, 22, 28–31*), Fourier resonance energy transfer (FRET) experiments were carried out. In a head-to-tail dimer, the Walker A domain of one subunit is expected to interact with the signature domain of the other. To determine such a conformation, a single-cysteine substitution was introduced within the Walker A [A45C(A)/C260S(B)] or ABC signature motif [Y140C(A)/C260S(B)] of DrrA. The expression levels of DrrA and DrrB proteins in both of these mutants were unaffected (data not shown). The membrane fractions prepared from strains containing these mutations were then labeled with either MIANS or NBD-Cl. Following incubation with either probe, the DrrAB proteins were immediately purified. For labeling in the membrane, the procedure mentioned in ref *32* was followed. MIANS and NBD-Cl are fluorophores that become fluorescent only on binding to cysteine residues within a protein. The fluorescent emission spectra were measured spectrofluorimetrically to determine whether binding of the probe to cysteines in DrrA took place. Data in Figure 3 (panels A and B) show that both A45C and Y140C could be labeled with either MIANS or NBD-Cl. Since the fluorescence emission spectrum of MIANS overlaps fairly well with the absorbance spectrum of NBD-Cl (*33*), MIANS and NBD-Cl form a good donor–acceptor pair. Once the labeling of DrrA with these probes was successfully achieved, we wanted to determine if the energy transfer would occur between them. If the DrrA dimer is a head-to-tail dimer, we would expect energy transfer between A45C-MIANS and Y140C-NBD-Cl. Thus, in this experiment, excitation was carried out at 322 nm for MIANS, while emission was carried out between 350 and 600 nm to be able to observe fluorescence emission of both MIANS and NBD-Cl. The data are shown in Figure 3E. When excitation is carried out at 322 nm, the MIANS-A45C protein shows an emission peak at 420 nm (panel E, curve 1) which is also seen in panel A (curve 1). NBD-Y140C gives no signal under these conditions (panel E, curve 2), as expected. When these proteins were mixed, excitation at 322 nm resulted in significant (~90%) quenching of the MIANS emission peak (panel E, curve 3). This quenching is simultaneously accompanied by an emission peak at 530 nm (panel E, curve 3) from NBD-Y140C. These data show that fluorescence energy transfer

Table 1: Doxorubicin Resistance of *E. coli* N43 Cells Expressing Different Mutations in DrrA and Wild-Type DrrB[a]

domain of DrrA	mutation	0 μg/mL doxorubicin	6 μg/mL doxorubicin	8 μg/mL doxorubicin	10 μg/mL doxorubicin
wild-type	C260	+++	+++	+++	++
Cys-less	C260S	+++	+++	+++	++
Walker A domain	A45C	+++	+++	+	+
Walker A domain	G44A	+++	+/−	−	−
Walker A domain	K47R	+++	−	−	−
Walker B domain	L160A	+++	−	−	−
Walker B domain	D164N	+++	−	−	−
Walker B domain	E165Q	+++	−	−	−
Q-loop domain	Y89C	+++	+++	++	+
Q-loop domain	S91C	+++	+++	++	+
Q-loop domain	Q88E	+++	++	+	−
Q-loop domain	Q88S	+++	−	−	−
Q-loop domain	Q88N	+++	+	−	−
Signature domain	Y140C	+++	+++	+/−	+/−
signature domain	S141R	+++	+	−	−
signature domain	G143S	+++	+	−	−
N-terminal tail (DrrB)	S23C	+++	++	++	++
double mutant	Y89C/S23C	+++	+++	++	++
double mutant	S91C/S23C	+++	++	++	++
vector only	pSU2718	+++	+/−	−	−

[a] N43 cells containing indicated plasmids were plated on M9 plates containing different concentrations of doxorubicin. The plates were incubated at 37 °C. Growth was scored after incubation for 24 h. Legend: +++, very good growth; ++, good growth; +, some growth; −, no growth.

occurred between MIANS bound to A45C and NBD-Cl bound to Y140C. Control experiments, where A45C-MIANS was mixed with A45C-NBD-Cl or Y140C-MIANS was mixed with Y140C-NBD-Cl, are shown in panels C and D of Figure 3, respectively. When excitation was carried out at 322 nm, the fluorescence property of either probe in these situations remained unaltered (curve 3), indicating that significant measurable energy transfer did not occur between two probes in the Walker A domains or the signature domains. These data indicate that the Walker A motif of one DrrA molecule lies in the proximity of the signature motif of another DrrA molecule in the DrrA dimer.

Characterization of Subunit Interactions by Use of Disulfide Cross-Linkers. The N-terminal cytoplasmic tail of DrrB, including residues 1–53, was previously shown by GMBS-mediated (cysteine-to-amine) cross-linking experiments to be involved in interaction with DrrA (*7*). To identify regions in DrrA that may be involved in interaction with the N-terminal region of DrrB, cysteine substitutions were introduced into DrrA. Wild-type DrrA contains no cysteine, while wild-type DrrB contains one at position 260, which was modified to a serine (*7*). The cysteine-less DrrAB proteins still conferred doxorubicin resistance to the same level seen in the wild-type system (Table 1). Cysteine substitutions in DrrA were then made in a plasmid already containing the S23C substitution in DrrB, or in the Cys-less DrrB background, unless indicated otherwise. The residues chosen for cysteine substitutions in DrrA were selected so that they were positioned either within or in the proximity of the conserved domains in DrrA, and (when possible) they would result in conservative changes. While 10 double mutants were originally constructed, five mutations showed significantly reduced levels of DrrA and DrrB expression and thus were not used for further investigation. The five remaining double-cysteine mutants [Y89C(A)/S23C(B), S91C(A)/S23C(B), S174C(A)/S23C(B), T195C(A)/S23C(B), and Y198C(A)/S23C(B)] were analyzed by cross-linking with a 0 Å disulfide cross-linker, CuPhe. Cross-linking between S23C in DrrB and a cysteine in DrrA is expected to result in a 65 kDa species. The data in Figure 4 show, that in two cysteine mutants, namely, Y89C(A)/S23C(B) and S91C(A)/S23C(B), both in the Q-loop region, a major cross-linked species migrating at 78 kDa (marked with an asterisk) was produced instead. The efficiency of cross-linking was almost in the range of 90% for Y89C. This species was seen only in the blots probed with the anti-DrrA antibody (Figure 4A) but was absent in the blots probed with the anti-DrrB antibody (Figure 4B). In addition, a minor 65 kDa species (also marked with an asterisk) was also produced, which could be detected by both anti-DrrA (Figure 4A) and anti-DrrB (Figure 4B) antisera, indicating that it is a complex of DrrA and DrrB. In the blot shown in Figure 4B (probed with the anti-DrrB antibody), we also see DrrB dimers in samples treated with CuPhe. This results from the presence of C260 in wild-type DrrB or S23C substitution of DrrB used in the rest of this experiment. Since DrrB dimers are produced in all cysteine variants tested (only C260 and S23C are shown in Figure 4), this species results from nonspecific association of DrrB monomers in the presence of a disulfide cross-linker. Nonspecific association of cysteine variants of DrrA is clearly not seen (Figure 4A); thus, we conclude that DrrB, being a membrane protein, is more prone to this kind of aggregation.

When another disulfide cross-linker, DTME, was used, we found that once again the major cross-linked species with Y89C DrrA corresponded to 78 kDa in size (Figure S3, lanes 3 and 4). Once again, a very high yield of the cross-linked species (varying between 70 and 90%) was obtained. To determine whether the 78 kDa cross-linked species was formed between two monomers of DrrA [Y89C(A)/Y89C DrrA] or between DrrA and DrrB [Y89C(A)/S23C(B)], two other variants of DrrB were tested. One contained C260 as the only cysteine in DrrB [Y89C(A)/C260(B)], and the other contained no cysteine [Y89C(A)/C260S(B)]. DTME-mediated disulfide cross-linking showed that the location of a cysteine in DrrB [whether S23C (Figure S3, panel A, lanes 3 and 4) or C260 (Figure S3, panel A, lanes 5 and 6)] made no difference to the Y89C-mediated disulfide cross-linking. Furthermore, the 78 kDa cross-linked species was formed even in the absence of a cysteine in DrrB (Figure S3, panel A, lanes 7 and 8), suggesting that the cross-linked species

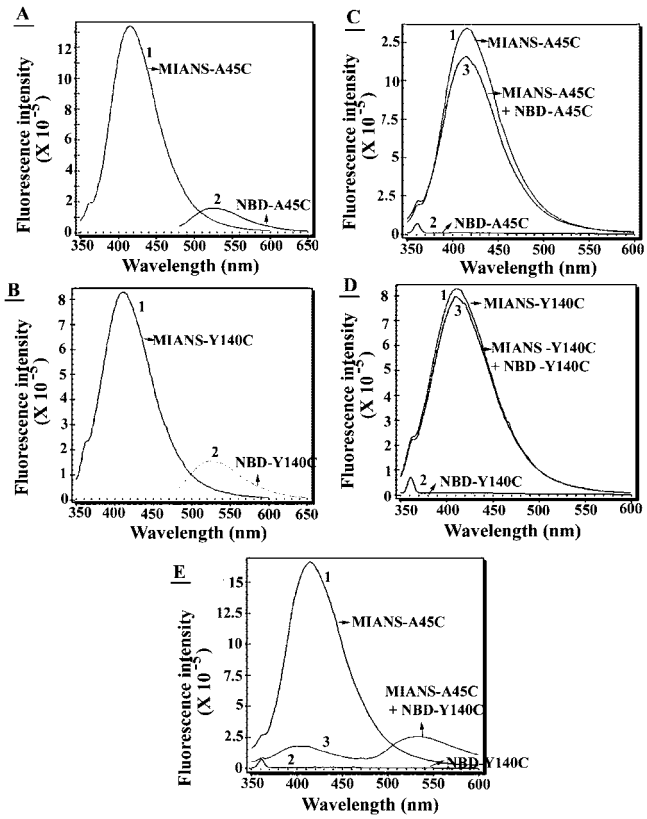

FIGURE 3: Fourier resonance energy transfer (FRET) analysis to determine the conformation of DrrA dimers. The membrane fractions prepared from cells containing A45C(A)/C260S(B) or Y140C(A)/C260S(B) were labeled with either MIANS or NBD-Cl. The labeled DrrAB proteins were purified as described in Experimental Procedures. (A and B) Fluorescence spectra for individual proteins labeled with MIANS (excitation at 322 nm; emission at 350–600 nm) or NBD (excitation at 465 nm; emission at 350–600 nm). (C) In separate reactions, A45C(A)/C260S(B) was labeled with either MIANS or NBD; 250 μL (approximately 100 μg) of each individually labeled proteins was then mixed. Excitation was carried out at 322 nm for MIANS, and emission was monitored between 350 and 600 nm. (D) In separate reactions, Y140C(A)/C260S(B) was labeled with either MIANS or NBD; 250 μL (approximately 100 μg) of individually labeled proteins was then mixed. Excitation was carried out at 322 nm for MIANS, and emission was monitored between 350 and 600 nm. (E) A45C(A)/C260S(B) labeled with MIANS was mixed with Y140C(A)/C260S(B) labeled with NBD-Cl; 250 μL (approximately 100 μg each) of each of these two labeled proteins were mixed. Excitation was carried out at 322 nm for MIANS, and emission was monitored between 350 and 600 nm. These experiments were repeated three times.

may be a homodimer of DrrA. We also found that the formation of this species was independent of the presence or absence of ATP (Figure S3, panel B, lanes 1–3). It should be mentioned here that either the Y89C or S91C substitution of DrrA or the S23C substitution of DrrB did not alter doxorubicin resistance conferred by the DrrAB proteins (Table 1).

To determine the exact composition of the 78 kDa cross-linked species and to verify that it represents the DrrA dimer, the DrrAB proteins were purified from the single-cysteine mutant [Y89C(A)/C260S(B)] cloned in a pET vector (Figure S4). The purified Y89C protein contained the 78 kDa species even without addition of the cross-linker (Figure S4, panel A, lane 9), indicating that the two cysteines are in the proximity of one another and were therefore spontaneously oxidized to yield a disulfide cross-linked species. The formation of the cross-linked species was further enhanced on addition of DTME (Figure S4, panel A, lane 10). The gel slice containing the 78 kDa species was excised from the gel shown in Figure S4 (panel A, lane 9) and subjected to SELDI analysis using the CIPHERGEN Protein Chip Technology, as described in Experimental Procedures. Analysis of the peptide map of the 78 kDa species showed that 96.4% of the peptides generated by the 78 kDa species matched that of the DrrA protein. Therefore, all of the above data together suggest that the 78 kDa species is a multimer, most likely a dimer, of DrrA. The DrrA monomer is 36.5 kDa in size; thus, the dimer should migrate at 73 kDa on SDS−PAGE. However, the cross-linked species migrates at 78 kDa. This may be due to the specific conformation of the dimer resulting from cross-linking. To determine if formation of the 78 kDa DrrA dimeric species is DrrB-dependent, purified DrrA or DrrAB proteins were subjected to DTME cross-linking (Figure S4, panel B). As reported earlier, both DrrA and DrrB proteins are dependent on each other for stability (*6*). The level of expression of DrrA in the absence of DrrB is ~50–60% of that of the DrrAB-containing system, while the expression of DrrB protein is undetectable in the absence of DrrA (*6*). The densitometric analysis of the monomeric and dimeric species seen in panel B of Figure S4 shows that while the yield of purified DrrA from the DrrA-alone system is half of that from the DrrAB system, the yield of the cross-linked 78 kDa species is almost 10-fold reduced, indicating that DrrB is required for efficient dimerization of DrrA.

Effect of ATP and ATPγS on Dimer Formation. To further characterize the effect of nucleotide binding on DrrA homodimer formation, purified cysteine-less DrrAB and Y89C(A)/C260S(B) proteins were incubated with ATP or the nonhydrolyzable analogue ATPγS. Since the purified Y89C DrrA protein spontaneously forms the 78 kDa species (shown in Figure S4, panel A, lane 9), the samples were first reduced with DTT to break up the disulfide bonds (Figure 5A, lane 1). On addition of DTME to this reduced protein, the 78 kDa species was again seen (Figure 5A, lane 4). Interestingly, addition of ATPγS to the purified protein, in the absence of DTME, was also seen to result in the formation of the 78 kDa species (Figure 5A, lane 3). However, addition of ATP to the Y89C protein (Figure 5A, lane 2) or ATPγS to the cysteine-less mutant did not induce dimerization (Figure 5A, lane 7). To determine the role of the nucleotide binding domain in Y89C-mediated dimerization, a K47R mutation in the Walker A domain was constructed in the existing Y89C(A)/C260S(B) background. K47R mutation completely abolishes binding of ATP to DrrA (Figure 2A). The resulting protein [Y89C,K47R(A)/C260S(B)] was purified and cross-linked with the disulfide cross-linker DTME (Figure 5B). The DrrA protein in this mutant failed to dimerize even in the presence of DTME even though it contained the Y89C mutation (Figure 5B, lanes 5 and 6). Further characterization was carried out by using E165Q, a mutation in the Walker B domain. Since E165Q binds ATP very well (Figure 2B, right panel), this mutation was introduced into the existing Y89C(A)/C260S(B) mutant. Y89C,E165Q(A)/C260S(B) formed disulfide cross-linked species in the presence of DTME (Figure 5C, lane 8), as seen with Y89C(A)/C260S(B). Furthermore, this protein also

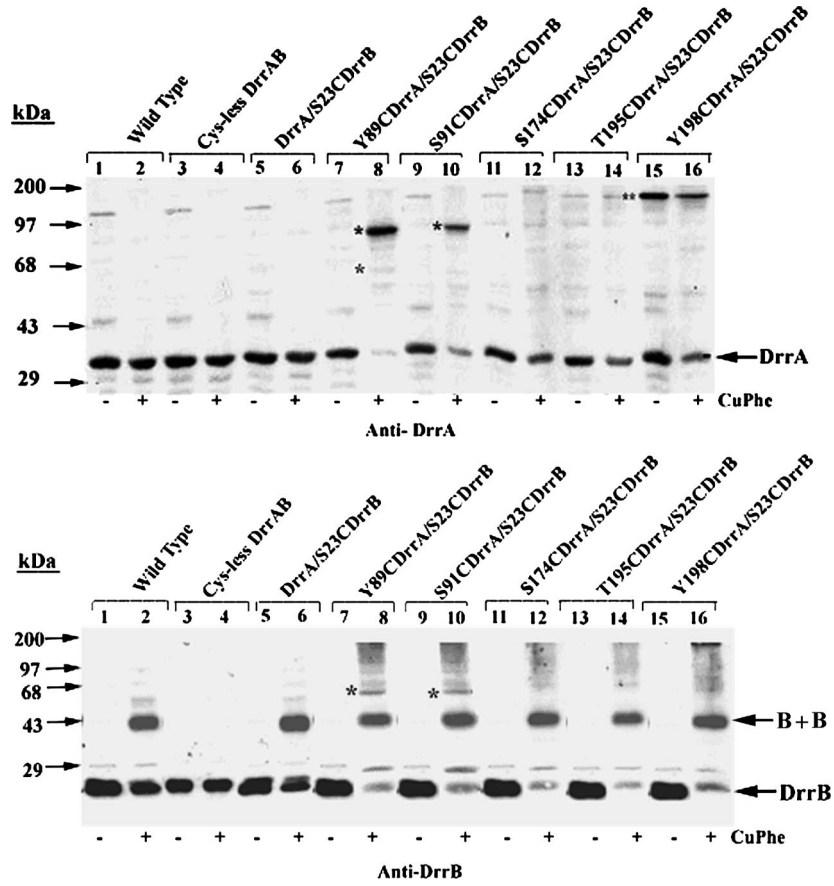

FIGURE 4: Copper phenanthroline-mediated disulfide cross-linking of DrrAB proteins. The cell membrane fractions were prepared and subjected to disulfide cross-linking using copper phenanthroline, as described in Experimental Procedures. The reaction was terminated by the addition of 25 μL of 4× nonreducing Laemmli sample buffer; 50 μg of protein was resolved by SDS−PAGE using 10% gels followed by Western blotting using anti-DrrA or anti-DrrB antibodies: lanes 1 and 2, wild-type DrrAB; lanes 3 and 4, cysteine-less DrrAB; lanes 5 and 6, (A)/S23C(B); lanes 7 and 8, Y89C(A)/S23C(B); lanes 9 and 10, S91C(A)/S23C(B); lanes 11 and 12, S174C(A)/S23C(B); lanes 13 and 14, T195C(A)/S23C(B); and lanes 15 and 16, Y198C(A)/S23C(B). Anti-DrrA antibodies in the top panel and anti-DrrB antibodies in the bottom panel. The minus and plus signs at the bottom of the lanes indicate the absence and presence of the cross-linker in the reaction, respectively. The migration of the protein standards is shown on the left. The location of the 78 kDa cross-linked species as well as the 65 kDa cross-linked species is marked with an asterisk. A much larger species seen in Y198C(A)/S23C(B) in both the absence and the presence of the cross-linker (two asterisks) was not characterized further in this study. These experiments were repeated three times.

showed significant dimerization on addition of either ATP or ATPγS, even without addition of DTME (Figure 5C, lanes 5–7). E165Q alone, in the absence of the Y89C mutation, did not show dimerization in the presence of DTME, ATP, or ATPγS (Figure 5C, lanes 1–4). Together, the data from panels B and C of Figure 5 suggest that an intact ATP binding Walker A domain is required for the formation of DrrA dimers and that the Y89C dimers can be held together either by the use of the disulfide cross-linker or by binding of ATPγS alone to the dimer interface, which will fix the dimer in one position. The averages of the ratio of cross-linked dimer to monomeric DrrA protein are plotted in a histogram shown in Figure S5.

Effect of DrrB on the Conformation of DrrA. As shown in the previous experiments, disulfide cross-linking using DrrAB containing one cysteine in DrrA [Y89C(A)/C260S(B)], or two cysteines, one each in DrrA and DrrB [Y89C(A)/S23C(B)], results predominantly in the 78 kDa DrrA homodimeric species, indicating that Y89C is in close contact with Y89C from another subunit of DrrA. A minor 65 kDa species, consisting of DrrA and DrrB, is also seen when S23C in DrrB is simultaneously present. To further characterize DrrA−DrrB and DrrA−DrrA interaction, a cysteine-to-amine cross-linker, GMBS (arm length of 7.3 Å), was used. GMBS cross-linking of six different cysteine substitutions in DrrA and wild-type DrrB was analyzed. These included A45C(A)/C260S(B), Y89C(A)/C260S(B), Y140C(A)/C260S(B), S174C(A)/C260S(B), T195C(A)/C260S(B), and Y198C(A)/C260S(B). Of these, only Y89C and Y140C, both in the helical domain of DrrA, showed cross-linking with GMBS. Moreover, they produced identical cross-linking patterns. Only the data obtained with GMBS cross-linking of Y89CDrrA are shown in Figure 6. In this experiment, (A)/S23C(B) served as a control. GMBS cross-linking of S23C with an amine in DrrA produces a major 65 kDa DrrA−DrrB species (Figure 6A,B, lanes 1 and 2), as also reported previously (*7*). Y89C(A)/C260S(B) exhibited a different cross-linking pattern, however (Figure 6A,B, lanes 3 and 4). Three cross-linked species were seen: a minor 65 kDa species and two major species of 78 and 100 kDa. The 65 kDa species corresponds to a heterodimer of A and B and is detected by both anti-DrrA (Figure 6A, lane 4) and anti-DrrB antisera (Figure 6B, lane 4), while the 78 kDa species is a homodimer of DrrA and is detected only by anti-DrrA antibodies (Figure 6A, lane 4) and not by anti-DrrB serum (Figure 6B, lane 4). The third 100 kDa species is again detected by anti-DrrA antibodies (Figure 6A, lane 4), but not by anti-DrrB antibodies (Figure 6B, lane 4). The significance of the 100 kDa species is not

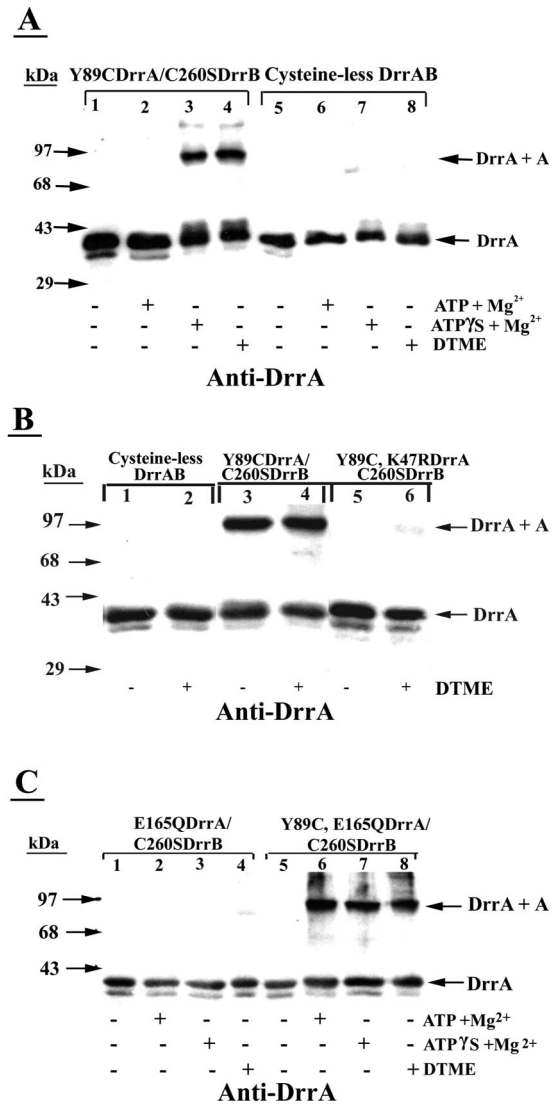

FIGURE 5: Effect of ATP and ATPγS on DrrA homodimer formation in Walker A and Walker B mutants. DrrAB proteins were purified as described in Experimental Procedures. Proteins used in panels A and C were reduced with 1 mM DTT and passed through a 10K Nanosep centrifugal column, whereas proteins used in panel B were used without reduction with DTT. The protein samples were incubated with ATP, ATPγS, or DTME cross-linker. The reactions were terminated by the addition of 4× nonreducing Laemmli sample buffer. Fifteen micrograms of each sample was analyzed by SDS−PAGE, followed by Western blotting using anti-DrrA antibodies. (A) Proteins were reduced with 1 mM DTT before incubation with ATP, ATPγS, or DTME: lanes 1–4, Y89C(A)/C260S(B); lanes 5–8, cysteine-less DrrAB. (B) Purified proteins were used without reduction with DTT: lanes 1 and 2, cysteine-less DrrAB; lanes 3 and 4, Y89C(A)/C260S(B); lanes 5 and 6, Y89C,K47R(A)/C260S(B). (C) Proteins were reduced with 1 mM DTT before incubation with ATP, ATPγS, or DTME: lanes 1–4, E165Q(A)/C260S(B); lanes 5–8, Y89C,E165Q(A)/C260S(B). The minus and plus signs at the bottom of the lanes indicate the absence and presence, respectively, of ATP, ATPγS, or the DTME cross-linker in the reaction mixture. The migration of the protein standards is shown on the left. The location of the 78 kDa cross-linked species is marked. These experiments were repeated three times. Quantitation was done as described in legend of Figure 2. The averages of the cross-linking efficiency are provided in Figure S5 as a histogram.

clear at this moment. Since it is not detected by anti-DrrB, it is likely that it represents a different conformation of the Y89C DrrA homodimer that has been doubly cross-linked through GMBS-mediated cysteine−amine cross-links, thus

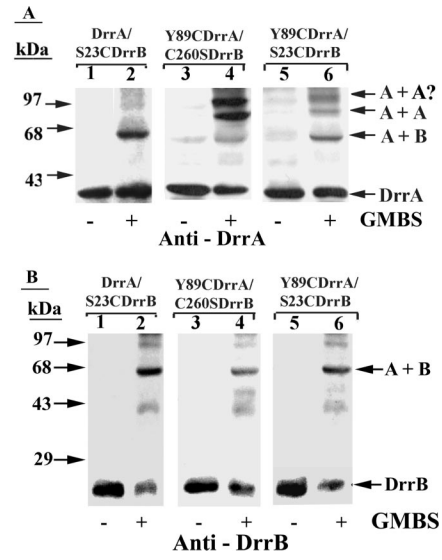

FIGURE 6: GMBS-mediated heterobifunctional cross-linking. The cell membrane fractions were prepared as described earlier. Cross-linking was carried out as described in Experimental Procedures. The reaction was terminated by the addition of 4× nonreducing Laemmli sample buffer; 50 μg of protein was resolved by SDS−PAGE, followed by Western blot analysis using anti-DrrA or anti-DrrB antibodies: lanes 1 and 2, (A)/S23C(B); lanes 3 and 4, Y89C(A)/C260S(B); lanes 5 and 6, Y89C(A)/S23C(B). Anti-DrrA antibodies in panel A and anti-DrrB antibodies in panel B. The location of the cross-linked species is marked as A + B, A + A, and A + A? This experiment was repeated three times.

resulting in a different mobility. The composition of this species will be analyzed further in the future studies. However, the most important conclusion that can be drawn from the GMBS cross-linking experiment shown in lanes 3 and 4 of Figure 6A is that once a cysteine is placed in the Q-loop/helical domain of DrrA, the predominant interaction is between DrrA monomers. This was also seen before with the disulfide cross-linkers (Figure 4). Since a minor 65 kDa DrrA−DrrB species is also produced, it indicates that the same region of DrrA is also involved in interaction with DrrB. Furthermore, GMBS cross-linking experiments also provided another interesting insight. It was noted that the presence of S23C (DrrB) simultaneously with Y89C (DrrA) interfered with the formation of the DrrA homodimers as well as the 100 kDa species (Figure 6A, lane 6), suggesting that the introduction of S23C into DrrB affects Y89C-mediated A−A interaction. Furthermore, these data also show that the three situations, S23C (lanes 1 and 2), Y89C (lanes 3 and 4), and Y89C/S23C (lanes 5 and 6), represent three different conformations of DrrA and DrrB.

The effect of S23C in DrrB on Y89C in DrrA was analyzed further by use of the disulfide cross-linkers of different arm lengths. Results obtained with three cross-linkers, CuPhe (0 Å), DTME (13.3 Å), and MTS (24.0 Å), are compared in Figure 7A. All three cross-linkers showed the formation of the 78 kDa cross-linked species with equal efficiency when Y89C(A)/C260S(B) was used (Figure 7A, lanes 1–4). Interestingly, however, when S23C is present in DrrB, MTS-mediated cross-linking between Y89C and Y89C is completely prevented (lane 9), even though cross-linking by CuPhe (lane 7) and DTME (lane 8) was unaffected. These data indicate that S23C did not prevent DrrA−DrrA interaction but somehow altered it so that it is not picked up by the long arm length cross-linker MTS. In the MTS-treated

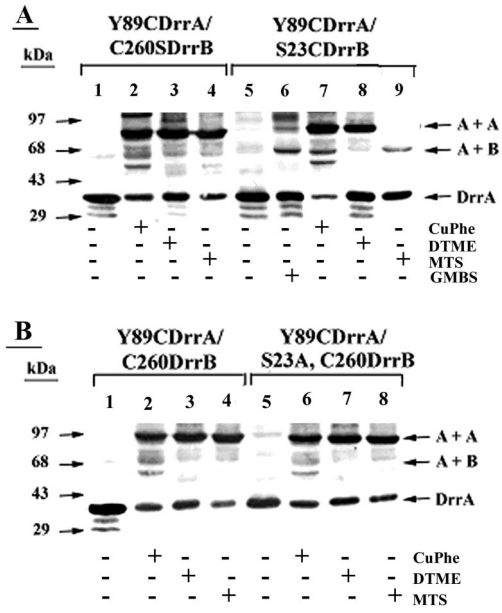

FIGURE 7: Use of disulfide cross-linkers of different arm lengths. The protocols for membrane preparation and cross-linking analyses were the same as described earlier. Three cross-linkers of different arm lengths were used. These include 3 mM/9 mM CuPhe (0 Å), 1 mM DTME (13.3 Å), or 0.2 mM MTS (24.0 Å); 50 μg of membrane protein was analyzed by SDS−PAGE, followed by analysis with anti-DrrA antibodies. (A) Lanes 1–4, Y89C(A)/C260S(B); lanes 5–9, Y89C(A)/S23C(B). (B) Lanes 1–4, Y89C(A)/C260S(B); lanes 5–8, Y89C(A)/S23A, C260(B). The minus and plus at the bottom of the lanes indicate the absence and presence of the cross-linker in the reaction, respectively. The migration of the protein standards is shown on the left. The experiment shown in Figure 7 was repeated four times and the averages are provided in Figure S6 as histograms.

samples containing Y89C and S23C, the only species seen is the 65 kDa (A + B) species (Figure 7A, lane 9), which is also seen in the CuPhe-treated samples (lane 7), and to a lesser extent in the DTME-treated samples. (A smaller species of 55 kDa, picked up by anti-DrrA antibodies in the CuPhe sample, has not been characterized further in this study.) The data shown in Figure 7 were quantitated, as described earlier for Figure 2. The averages of cross-linked dimer/monomeric DrrA protein are plotted in a histogram shown in Figure S6.

To determine if the presence of any other cysteine in DrrB could have a similar inhibitory effect on Y89C−Y89C cross-linking, Y89C(A)/C260(B) was tested. Data in Figure 7B (lanes 1–4) show that MTS-mediated Y89C−Y89C cross-linking was not prevented by C260. Thus, this effect was specific to S23C (N-terminal tail) of DrrB. Furthermore, if S23C in DrrB is replaced by S23A, once again MTS-mediated Y89C−Y89C cross-linking occurs normally (Figure 7B, lanes 5–8), indicating that a cysteine residue at position 23 in DrrB is required for this effect.

DISCUSSION

A major unresolved question that intrigues investigators in the field of ABC transporters is the mechanism by which their nucleotide binding domains interact with the membrane domains, a step essential for transduction of energy to bring about import or export. In the ABC drug transporter DrrAB, the NBD and the TMD are present on separate subunits but are tightly coupled for their function and stability (*6*). Recent efforts have provided some important insights into the molecular basis of subunit interaction, especially with regard to DrrB (*7*). The focus of this study was DrrA. We show here that the Q-loop region of DrrA plays an important role in producing the closed conformation of the nucleotide binding domains. Furthermore, it is also involved in mediating interactions between the NBD and the transmembrane subunit DrrB. The critical role played by the Q-loop in the function of ABC transporters has been recognized before in structural studies as well as biochemical studies (*24, 34–38*). The results obtained in this study strengthen previous observations and extend them further by (1) showing that the Q-loops from opposing subunits of DrrA move much closer together in the closed conformation and (2) providing evidence for communication between the Q-loop of DrrA and the TMD via the N-terminus of DrrB. The model in Figure 8 presents this information in the context of information already available in literature on other ABC proteins.

Previous studies from this laboratory have shown that in the resting state of the complex DrrA is in contact with DrrB. By using DTSSP, a general amine-to-amine cross-linker, only a heterodimeric species consisting of DrrA and DrrB was seen (*6*). Further, GMBS (a cysteine-to-amine cross-linker) experiments showed that residues in the N-terminal cytoplasmic tail of DrrB (residues 1–53) interact with DrrA (*7*). These results imply that in the resting state (represented as A−B in Figure 8) DrrA is predominantly in contact with DrrB and not another monomer of DrrA. In this study, we show that a cysteine substitution (Y89C or S91C) in the Q-loop of DrrA produces a conformational switch from A−B to the A−A homodimeric state.

Dimerization of the nucleotide binding domains is an important step in the catalytic mechanism of ABC transporters (*10, 11, 16, 18, 19, 22*). Since hydrolysis of ATP immediately returns the protein to the open conformation, the dimeric state is transient and thus is difficult to identify in solution or in the crystalline state. In some proteins (for example, MJ0796), mutation of the catalytic glutamate in Walker B was shown to enhance the stability of the dimer and was essential for crystallization of the protein in the dimeric state (*39*). In this study, we show that the Y89C or S91C substitution in the Q-loop traps DrrA in the dimeric conformation, suggesting that the Q-loop region is present at the interface of two monomers and is actively involved in dimerization of DrrA. We also propose that the Y89C-induced conformation of DrrA resembles the closed state, which normally results from binding of ATP to the ABC proteins (*10, 11, 16, 18, 19, 22*). In fact, Y89C-mediated disulfide cross-linking of DrrA monomers was independent of ATP binding so that 70–90% of the Y89C protein was already in the dimeric state without addition of ATP. Nevertheless, an intact ATP binding (Walker A) domain was required for achieving this conformation; specifically, the K47R mutation in the Walker A domain was found to be trapped in the open state, as proposed for the signature mutant in MalK and the Walker A mutant in Pgp (*24, 40*). We also found that on addition of a nonhydrolyzable ATP analogue ATPγS to Y89C (containing a wild-type Walker A domain), a stable DrrA dimer was produced even in the absence of the cross-linker, indicating that the Y89C−Y89C contact is sensitive to binding of ATP or ATPγS so that the Y89C dimer can be stabilized either by the disulfide cross-linker

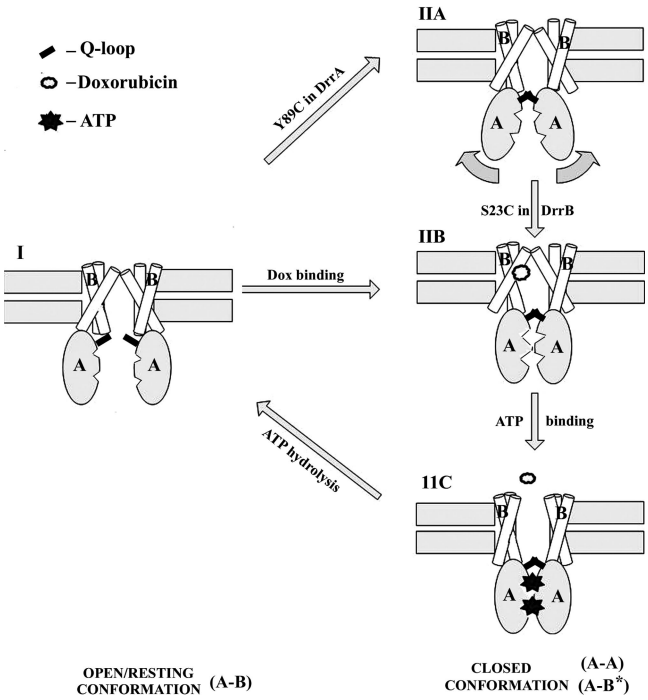

FIGURE 8: Model showing different conformations of DrrA and DrrB involved in the mechanism of doxorubicin efflux by the DrrAB pump. The model depicted here is based on analyses of Y89C and S23C substitutions in DrrA and DrrB, respectively. The resting state complex of DrrA and DrrB (Confo. I, represented as A−B) is shown on the left. This state was previously identified through DTSSP and GMBS cross-linking experiments (*6, 7*). In this state, the DrrA monomers are away from each other, and the primary interaction occurs between the N-terminal cytoplasmic tail of DrrB and an unidentified region of DrrA (*7*). Y89C substitution in DrrA changes the conformation to that resembling the closed conformation (Confo. IIA), as seen in disulfide cross-linking experiments presented in this study. In this conformation, the two Q-loops are close together (A−A), and they also form transient contacts with the N-terminal tail of DrrB (represented as A−B*). The Y89C−Y89C contact in this conformation is flexible (shown as a moving arrow); however, the simultaneous presence of S23C in DrrB produces a more rigid, closed conformation (Confo. IIB). We propose that this conformation resembles the conformation resulting from binding of doxorubicin to wild-type DrrAB, which is competent to bind ATP (*2*). Previous studies conducted in this laboratory showed that binding of ATP to DrrA occurs only when DrrA is in a complex with DrrB (*6*), and, furthermore, ATP binding to DrrA is stimulated by doxorubicin binding (*2, 6*). Binding of ATP to this conformation then serves as the power stroke (Confo. IIC) for efflux of doxorubicin. Hydrolysis of ATP subsequently returns the pump to the resting state. It should be mentioned here that the Confo. IIC shown in this model is not based on direct information available with the DrrAB proteins but is based on what is generally proposed in the literature. In fact, whether ATP binding or ATP hydrolysis serves as the power stroke in ABC proteins is still an open question (as discussed in ref *11*).

acting directly on the Q-loop or by binding of ATPγS to the interface of the dimer. Together, these data imply that the Y89C dimeric conformation indeed resembles the closed state, previously identified by crystal structure analysis of various ABC proteins (*11, 19*). Information gleaned from the MalK crystal structure specifically shows that the Q-loops of MalK move much closer together in the closed state and that the distance between His89 residues in the Q-loops from opposing subunits changes from 52.5 Å (open) to 27.2 Å (closed) (*19*). The most recent biochemical study from Schneider's group on the maltose system also strengthens the data and interpretations presented in this study both in terms of the distance between the Q-loops of MalK and in terms of trapping of MalK in the open or closed state (*24*). A homology model of the DrrA dimer based on the published MalK-ATP structure (*19*) shows that the structure of the ATP binding pocket in DrrA and MalK is very similar. Specifically, the distances between the conserved glutamines of two Q-loops from the opposing subunits in DrrA and MalK were seen to be 8.19 and 8.46 Å, respectively. Furthermore, DrrA was also modeled on the basis of the published structure of HlyB in both the ATP-bound and the ATPMg-bound form. The distance between the conserved glutamines was further reduced in the ATP-Mg (4.48 Å) form as compared to in the ATP form (8.89 Å) in DrrA, which is also seen in HlyB (*41, 42*).

Another aspect of the work described in this study involves interaction between the Q-loop of DrrA and the N-terminal cytoplasmic tail of DrrB. When S23C in the N-terminus of DrrB is simultaneously present along with Y89C in DrrA, a species corresponding to the heterodimer of DrrA and DrrB (65 kDa) is also observed, although the major interaction is between two DrrA monomers. Since Y89C represents the dimeric state of DrrA, the S23C−Y89C contact appears to be specific to the closed state and is represented as A−B* in Figure 8. (We believe that the A−B* conformation is different from the A−B conformation described earlier, even though both involve the N-terminal tail region of DrrB. This question will be resolved in future studies.) What might be the significance of the contacts between the S23 region (N-terminal cytoplasmic tail) in DrrB and the Q-loop of DrrA? According to the prevalent models based on crystal structures of HisP, MalK, and BtuCD, the flexible nature of the Q-loop allows the transition of the NBDs from the open to the closed state, and at the same time, it allows it to act as a relay of conformational changes between the nucleotide binding domain and the transmembrane domain (*19, 22, 43*).

On the basis of our own data presented here, we propose that the interaction between the S23 region of DrrB and the Q-loop of DrrA is involved in communication of conformational changes between DrrA and DrrB. Interestingly, substituting the S23 residue (DrrB) with S23C produces a significant effect on the behavior of Y89C in DrrA. This effect becomes evident only when different arm length disulfide cross-linkers are employed. As shown in the Results, DrrA (Y89C) can be cross-linked with high efficiency by linkers varying in length from 0 Å (CuPhe) to 24 Å (MTS). When S23C is simultaneously present in DrrB, the results are strikingly different: CuPhe and DTME (13.3 Å) can still cross-link DrrA and produce DrrA homodimers very well, but MTS is now not able to do so. These data indicate that placing a cysteine in this region of DrrB produces a conformational change in the helical domain of DrrA. It seems reasonable to suggest that it produces a more rigid conformation of DrrA so that Y89C can still be cross-linked with zero or short arm length cross-linkers but not with the long arm length linker MTS. This leads us to propose that the two Y89C residues (or the Q-loops) from opposing monomers are in flexible contact (Figure 8, Confo. IIA) until a conformational change in DrrB (produced by the S23C substitution here) produces a change in DrrA which fixes it in one position (Confo. IIB). The overall effect of this conformation of DrrB seems to be to facilitate the closed conformation of DrrA. This observation is consistent with

earlier findings, namely, that the isolated ABC domains do not form stable homodimers even in the presence of Mg-ATP or nonhydrolyzable analogues, indicating that interaction with the TM domains is required for stable association (*16*). Previous studies from this laboratory have also shown that DrrA binds ATP only when it is in complex with DrrB (*6*), further strengthening the idea that DrrB facilitates the closed conformation of DrrA. Since S23C lies in the region of interaction between DrrA and DrrB (*24*), the effect seen in this study is likely to be physiologically significant and thus may provide clues about the path of transmission of conformational changes from DrrB to DrrA. One situation where events in DrrB will be transmitted to DrrA is substrate binding to DrrB. We have shown before that doxorubicin binding to DrrB produces a significant enhancement of binding of ATP to DrrA (*6*). It can thus be speculated that doxorubicin binding to DrrB produces a conformational change in the N-terminal tail of DrrB which is then transmitted to the helical domain of DrrA (Confo. IIC). Is it possible then that the S23C substitution in the N-terminal tail of DrrB mimics the effect of substrate binding to DrrB? Such a model is consistent with earlier proposals that substrate binding to the TMD is signaled to the NBDs, which then results in their closing (*44*).

In this study, the role of the Q-loop region in formation of the closed conformation of the nucleotide binding domain has been clearly elucidated. Furthermore, the long-range effects of conformational changes in DrrB on DrrA are very intriguing and could provide important insights into the mechanism by which DrrA and DrrB communicate. In our future studies, we would like to further understand how DrrB influences DrrA and how the Q-loop region is involved in communication between the NBD and the TMD.

SUPPORTING INFORMATION AVAILABLE

Quantitation of incorporation of [α-^{32}P]ATP into wild type DrrA and mutants (Figure S1), competition of [α-^{32}P]ATP incorporation by excess unlabeled ATP (Figure S2), DTME-mediated disulfide cross-linking of Y89C (DrrA) (Figure S3), purification of DrrA and DrrAB proteins and DTME cross-linking (Figure S4), quantitation of the efficiency of disulfide cross-linking of Walker A and Walker B mutants (Figure S5), and quantitation of the efficiency of disulfide cross-linking by different arm length cross-linkers (Figure S6). This material is available free of charge via the Internet at http://pubs.acs.org.

REFERENCES

1. Guilfoile, P. G., and Hutchinson, C. R. (1991) A bacterial analog of the mdr gene of mammalian tumor cells is present in *Streptomyces peucetius*, the producer of daunorubicin and doxorubicin. *Proc. Natl. Acad. Sci. U.S.A. 88*, 8553–8557.
2. Kaur, P. (1997) Expression and characterization of DrrA and DrrB proteins of *Streptomyces peucetius* in *Escherichia coli*: DrrA is an ATP binding protein. *J. Bacteriol. 179*, 569–575.
3. Gottesman, M. M., and Pastan, I. (1993) Biochemistry of multidrug resistance mediated by the multidrug transporter. *Annu. Rev. Biochem. 62*, 385–427.
4. Senior, A. E. (1998) Catalytic mechanism of P-glycoprotein. *Acta Physiol. Scand. Suppl. 643*, 213–218.
5. Sauna, Z. E., Smith, M. M., Muller, M., Kerr, K. M., and Ambudkar, S. V. (2001) The mechanism of action of multidrug-resistance-linked P-glycoprotein. *J. Bioenerg. Biomembr. 33*, 481–491.
6. Kaur, P., and Russell, J. (1998) Biochemical coupling between the DrrA and DrrB proteins of the doxorubicin efflux pump of *Streptomyces peucetius*. *J. Biol. Chem. 273*, 17933–17939.
7. Kaur, P., Rao, D. K., and Gandlur, S. M. (2005) Biochemical characterization of domains in the membrane subunit DrrB that interact with the ABC subunit DrrA: Identification of a conserved motif. *Biochemistry 44*, 2661–2670.
8. Gandlur, S. M., Wei, L., Levine, J., Russell, J., and Kaur, P. (2004) Membrane topology of the DrrB protein of the doxorubicin transporter of *Streptomyces peucetius*. *J. Biol. Chem. 279*, 27799–27806.
9. Diederichs, K., Diez, J., Greller, G., Muller, C., Breed, J., Schnell, C., Vonrhein, C., Boos, W., and Welte, W. (2000) Crystal structure of MalK, the ATPase subunit of the trehalose/maltose ABC transporter of the archaeon *Thermococcus litoralis*. *EMBO J. 19*, 5951–5961.
10. Yuan, Y. R., Blecker, S., Martsinkevich, O., Millen, L., Thomas, P. J., and Hunt, J. F. (2001) The crystal structure of the MJ0796 ATP-binding cassette. Implications for the structural consequences of ATP hydrolysis in the active site of an ABC transporter. *J. Biol. Chem. 276*, 32313–32321.
11. Smith, P. C., Karpowich, N., Millen, L., Moody, J. E., Rosen, J., Thomas, P. J., and Hunt, J. F. (2002) ATP binding to the motor domain from an ABC transporter drives formation of a nucleotide sandwich dimer. *Mol. Cell 10*, 139–149.
12. Schmitt, L., Benabdelhak, H., Blight, M. A., Holland, I. B., and Stubbs, M. T. (2003) Crystal structure of the nucleotide-binding domain of the ABC-transporter haemolysin B: Identification of a variable region within ABC helical domains. *J. Mol. Biol. 330*, 333–342.
13. Verdon, G., Albers, S. V., Dijkstra, B. W., Driessen, A. J., and Thunnissen, A. M. (2003) Crystal structures of the ATPase subunit of the glucose ABC transporter from *Sulfolobus solfataricus*: Nucleotide-free and nucleotide-bound conformations. *J. Mol. Biol. 330*, 343–358.
14. Hung, L. W., Wang, I. X., Nikaido, K., Liu, P. Q., Ames, G. F., and Kim, S. H. (1998) Crystal structure of the ATP-binding subunit of an ABC transporter. *Nature 396*, 703–707.
15. Gaudet, R., and Wiley, D. C. (2001) Structure of the ABC ATPase domain of human TAP1 the transporter associated with antigen processing. *EMBO J. 20*, 4964–4972.
16. Karpowich, N., Martsinkevich, O., Millen, L., Yuan, Y. R., Dai, P. L., MacVey, K., Thomas, P. J., and Hunt, J. F. (2001) Crystal structures of the MJ1267 ATP binding cassette reveal an induced-fit effect at the ATPase active site of an ABC transporter. *Structure 9*, 571–586.
17. Davidson, A. L., and Chen, J. (2004) ATP-binding cassette transporters in bacteria. *Annu. Rev. Biochem. 73*, 241–268.
18. Hopfner, K. P., Karcher, A., Shin, D. S., Craig, L., Arthur, L. M., Carney, J. P., and Tainer, J. A. (2000) Structural biology of Rad50 ATPase: ATP-driven conformational control in DNA double-strand break repair and the ABC-ATPase superfamily. *Cell 101*, 789–800.
19. Chen, J., Lu, G., Lin, J., Davidson, A. L., and Quiocho, F. A. (2003) A tweezers-like motion of the ATP-binding cassette dimer in an ABC transport cycle. *Mol. Cell 12*, 651–661.
20. Lewis, H. A., Buchanan, S. G., Burley, S. K., Conners, K., Dickey, M., Dorwart, M., Fowler, R., Gao, X., Guggino, W. B., Hendrickson, W. A., Hunt, J. F., Kearins, M. C., Lorimer, D., Maloney, P. C., Post, K. W., Rajashankar, K. R., Rutter, M. E., Sauder, J. M., Shriver, S., Thibodeau, P. H., Thomas, P. J., Zhang, M., Zhao, X., and Emtage, S. (2004) Structure of nucleotide-binding domain 1 of the cystic fibrosis transmembrane conductance regulator. *EMBO J. 23*, 282–293.
21. Lewis, H. A., Zhao, X., Wang, C., Sauder, J. M., Rooney, I., Noland, B. W., Lorimer, D., Kearins, M. C., Conners, K., Condon, B., Maloney, P. C., Guggino, W. B., Hunt, J. F., and Emtage, S. (2005) Impact of the ΔF508 mutation in first nucleotide-binding domain of human cystic fibrosis transmembrane conductance regulator on domain folding and structure. *J. Biol. Chem. 280*, 1346–1353.
22. Locher, K. P., Lee, A. T., and Rees, D. C. (2002) The *E. coli* BtuCD structure: A framework for ABC transporter architecture and mechanism. *Science 296*, 1091–1098.
23. Dawson, R. J., and Locher, K. P. (2006) Structure of a bacterial multidrug ABC transporter. *Nature 443*, 180–185.
24. Daus, M. L., Grote, M., Muller, P., Doebber, M., Herrmann, A., Steinhoff, H. J., Dassa, E., and Schneider, E. (2007) ATP-driven MalK Dimer Closure and Reopening and Conformational Changes

of the "EAA" Motifs Are Crucial for Function of the Maltose ATP-binding Cassette Transporter (MalFGK2). *J. Biol. Chem. 282*, 22387–22396.
25. Nakamura, H., Tojo, T., and Greenberg, J. (1975) Interaction of the expression of two membrane genes, acrA and plsA, in *Escherichia coli* K-12. *J. Bacteriol. 122*, 874–879.
26. Sambrook, J., Fritsch, E. F., and Maniatis, T. (1989) *Molecular Cloning: A Laboratory Manual*, 2nd ed., Cold Spring Harbor Laboratory Press, Plainview, NY.
27. Miller, J. (1992) *Experiments in Molecular Genetics*, Cold Spring Harbor Laboratory Press, Plainview, NY.
28. Fetsch, E. E., and Davidson, A. L. (2002) Vanadate-catalyzed photocleavage of the signature motif of an ATP-binding cassette (ABC) transporter. *Proc. Natl. Acad. Sci. U.S.A. 99*, 9685–9690.
29. Loo, T. W., and Clarke, D. M. (1995) P-glycoprotein. Associations between domains and between domains and molecular chaperones. *J. Biol. Chem. 270*, 21839–21844.
30. Dalmas, O., Do Cao, M. A., Lugo, M. R., Sharom, F. J., Di Pietro, A., and Jault, J. M. (2005) Time-resolved fluorescence resonance energy transfer shows that the bacterial multidrug ABC half-transporter BmrA functions as a homodimer. *Biochemistry 44*, 4312–4321.
31. Guo, X., Chen, X., Weber, I. T., Harrison, R. W., and Tai, P. C. (2006) Molecular basis for differential nucleotide binding of the nucleotide-binding domain of ABC-transporter CvaB. *Biochemistry 45*, 14473–14480.
32. Liu, R., and Sharom, F. J. (1998) Proximity of the nucleotide binding domains of the P-glycoprotein multidrug transporter to the membrane surface: A resonance energy transfer study. *Biochemistry 37*, 6503–6512.
33. Qu, Q., and Sharom, F. J. (2001) FRET analysis indicates that the two ATPase active sites of the P-glycoprotein multidrug transporter are closely associated. *Biochemistry 40*, 1413–1422.
34. Hunke, S., Mourez, M., Jehanno, M., Dassa, E., and Schneider, E. (2000) ATP modulates subunit-subunit interactions in an ATP-binding cassette transporter (MalFGK2) determined by site-directed chemical cross-linking. *J. Biol. Chem. 275*, 15526–15534.
35. Dalmas, O., Orelle, C., Foucher, A. E., Geourjon, C., Crouzy, S., Di Pietro, A., and Jault, J. M. (2005) The Q-loop disengages from the first intracellular loop during the catalytic cycle of the multidrug ABC transporter BmrA. *J. Biol. Chem. 280*, 36857–36864.
36. Mourez, M., Jehanno, M., Schneider, E., and Dassa, E. (1998) In vitro interaction between components of the inner membrane complex of the maltose ABC transporter of *Escherichia coli*: Modulation by ATP. *Mol. Microbiol. 30*, 353–363.
37. Wilken, S., Schmees, G., and Schneider, E. (1996) A putative helical domain in the MalK subunit of the ATP-binding-cassette transport system for maltose of *Salmonella typhimurium* (MalFGK2) is crucial for interaction with MalF and MalG. A study using the LacK protein of *Agrobacterium radiobacter* as a tool. *Mol. Microbiol. 22*, 655–666.
38. Mourez, M., Hofnung, M., and Dassa, E. (1997) Subunit interactions in ABC transporters: A conserved sequence in hydrophobic membrane proteins of periplasmic permeases defines an important site of interaction with the ATPase subunits. *EMBO J. 16*, 3066–3077.
39. Moody, J. E., Millen, L., Binns, D., Hunt, J. F., and Thomas, P. J. (2002) Cooperative, ATP-dependent association of the nucleotide binding cassettes during the catalytic cycle of ATP-binding cassette transporters. *J. Biol. Chem. 277*, 21111–21114.
40. Tombline, G., Muharemagic, A., White, L. B., and Senior, A. E. (2005) Involvement of the "occluded nucleotide conformation" of P-glycoprotein in the catalytic pathway. *Biochemistry 44*, 12879–12886.
41. Zaitseva, J., Jenewein, S., Jumpertz, T., Holland, I. B., and Schmitt, L. (2005) H662 is the linchpin of ATP hydrolysis in the nucleotide-binding domain of the ABC transporter HlyB. *EMBO J. 24*, 1901–1910.
42. Zaitseva, J., Oswald, C., Jumpertz, T., Jenewein, S., Wiedenmann, A., Holland, I. B., and Schmitt, L. (2006) A structural analysis of asymmetry required for catalytic activity of an ABC-ATPase domain dimer. *EMBO J. 25*, 3432–3443.
43. Jones, P. M., and George, A. M. (2002) Mechanism of ABC transporters: A molecular dynamics simulation of a well characterized nucleotide-binding subunit. *Proc. Natl. Acad. Sci. U.S.A. 99*, 12639–12644.
44. Davidson, A. L., Shuman, H. A., and Nikaido, H. (1992) Mechanism of maltose transport in *Escherichia coli*: Transmembrane signaling by periplasmic binding proteins. *Proc. Natl. Acad. Sci. U.S.A. 89*, 2360–2364.

BI701699A